Proceedings World Geothermal Congress 2020+1
Reykjavik, Iceland, April - October 2021

Play-Fairway Analysis for Deep Geothermal Resources in Switzerland

Benoît Valley and Stephen A. Miller

Centre for Hydrogeology and Geothermics (CHYN), University of Neuchâtel, Switzerland

benoit.valley@unine.ch, stephen.miller@unine.ch

Keywords: Play-fairway analysis; Switzerland; Molasse basin

ABSTRACT

Switzerland initiated an energy transition plan for a massive development of renewable energy sources in response to climate change challenges and the decision to shut down nuclear power plants. Geothermal energy represents one component of this transition, with energy scenarios planning for more than 5% of the Swiss electricity demand produced from geothermal energy by 2050. Geothermal energy potentially provides base-load electricity supply, while also contributing to direct and indirect heat supply for replacing fossil fuels, and thus reducing greenhouse gas emissions.

In response to this initiative, the Swiss Geological Survey (swisstopo) compiles information of the subsurface relevant for deep geothermal energy, including well data, seismic data interpretation of major stratigraphic horizons and faults, heat flux maps, thermal models of the underground, and geothermal potential studies. Access to this database provides opportunities for reviewing the geothermal potential of Switzerland using a quantitative play-fairway approach.

In this contribution, we first review the available data sets and propose conceptual classifications of geological and structural settings favorable for deep-seated fluid circulation in Switzerland. We use the available data to determine best-estimate stress models, which are then used to compute slip and dilation tendency on the main faults identified in the database. We also combine all available information to provide quantitative mapping of the fairway score (favorability maps) for geothermal exploration. Model resolution does not yet capture local effects relevant for specific project development, but does identify general trends at the scale of Switzerland. Currently, this approach provides best estimate models for the currently available data, and will be refined and better-resolved with the acquisition and implementation of future data.

1 INTRODUCTION

The energy transition taking place worldwide aims to mitigate greenhouse gas emissions, and Switzerland is following this trend with a vote in 2017 for an energy transition plan called "energy strategy 2050." This strategy also includes shutting down Swiss nuclear plants that account for 40% of current power production, with renewable energy resources filling this gap. With the capability of providing base load supply, geothermal energy potentially plays an important role in the electricity production mix, in addition to replacing hydrocarbons for heating and hot water in buildings. Currently, oil and gas provide 60% of the energy needs in Switzerland.

In the energy strategy 2050, geothermal should cover 5% of the Swiss electrical power supply, which translates to constructing at least 50 geothermal power plants. Switzerland has not been extensively explored for oil and gas, so targeting deep boreholes remains a challenge because knowledge on the deep underground is limited. A series of measures have been put in place to support developing geothermics, including compiling as much information as possible of the deep underground relevant to geothermics. The Swiss Geological Survey compiled such information in 3D for the Swiss Molasse basin including well data, seismic data interpretation of major stratigraphic horizons and faults (Allenbach et al. 2017), heat flux maps, thermal models of the underground, and geothermal potential studies.

In this contribution, we want to valorize this new compilation of data in order to propose geothermal fairway analyses at the basin scale. The current potential targets in Switzerland are defined in a general conceptual manner, but lack details on the characterization and an identification of the actual target positions. The conceptual targets (Figure 1) for electricity production (using 120°C in situ temperature lower limit) are generally deeper than 2600 m, while for direct-use heating (80 °C in-situ temperature threshold) target formations are at about 1400 m or deeper.

In the sedimentary basin, some formations are known as regional aquifers and may have sufficient natural permeability and porosity to be exploited as geothermal reservoirs, although lateral facies changes can largely affect the hydrogeological characteristics of these formations (Adams and Diamond 2019). In addition, secondary porosity and permeability developed through fracturing processes and/or karstification provide generally an important control on flow path in these formations. Natural fracturing is enhanced in rock mass volumes undergoing localized deformation such as fault zones and fold hinges, while karstification is a dissolution process requiring fluid flow in geochemical disequilibrium. Karstification occurs in carbonate rock mases near-surface (epigenic karsts) and driven by rain recharge, or through circulation of deep fluids (hypogenic karsts). Reconstructing the hydrodynamical conditions driving karstification remains a challenge.

In the basement rocks, secondary porosity and permeability through faulting and fracturing is required to facilitate fluid flow. The top of the basement as been exposed at surface prior to the onset of sedimentation and can present along the first 10s to couple of 100s m unloading fracturing pattern and weathering profiles that can be favorable to fluid flow. Deeper in the basement, the presence of enhanced fracturing related to faulting is required to develop sufficient permeability.

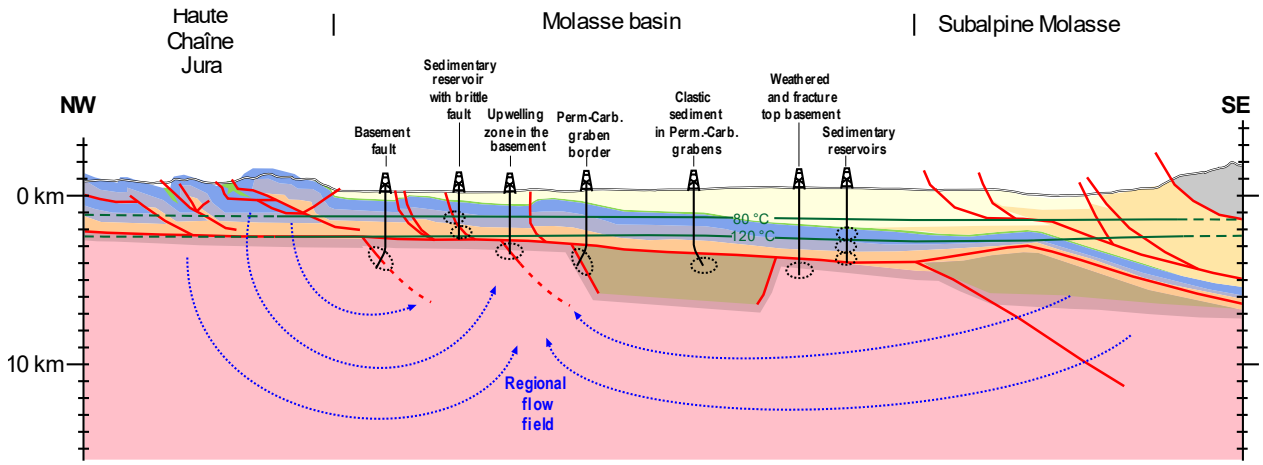

Figure 1 : Cross-section through the Swiss plateau, after Burkhard and Sommaruga (1998), showing conceptual targets for deep geothermal energy production.

In order to localize these potential targets, we adopt the general approach proposed by Siler and Faulds (2013) by identifying features in the data that are either favorable or unfavorable for geothermal development, then score and combine them to generate geothermal fairway favorability maps. Before presenting the details of the approach, we describe the data sets used in our analyses. We then discuss the fairways scores for each element of our analyses and the consolidated favorability index. These results should be considered as a first appraisal of the favorability for deep geothermal development at the Swiss Molasse basin scale, which will evolve as more detailed data and analysis are integrated.

2 DATASET

2.1 Mechanical and Hydro-Stratigraphy

The lithology primarily controls the hydrological and mechanical properties of the underground. The lithological column below the Swiss Molasse Basin (Figure 2) is modified after Chevalier et al. (2010) and we follow their approach by converting the lithological column to a hydrostratigraphy, identifying aquifer and aquiclude formations. We also define a mechanical stratigraphy based on the formation stiffness and brittleness following the work of Hergert et al. (2015), which is necessary to run stress models and assess formation fracturing. The horizons modelled in the GeoMol model of Swisstopo (version GeolMol18, Allenbach et al. 2017) are also listed in Figure 2.

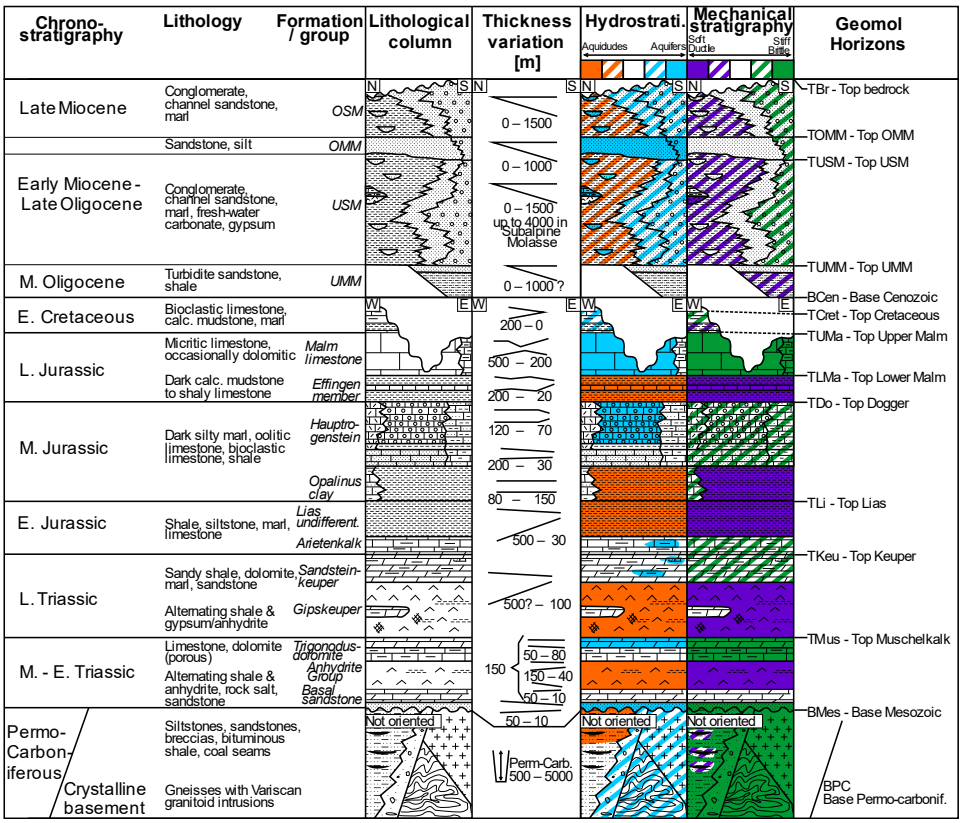

Figure 2 : Stratigraphic column below the swiss plateau and interpreted hydro- and mechanical stratigraphy (modified after Chevalier et al. 2010).

2.2 Structures

Figure 3 shows the GeoMol dataset available for our analyses and includes more than 550 fault surfaces (version GeolMol18, Allenbach et al. 2017). The heterogeneous fault data include various fault types (e.g. strike-slip, thrust, etc.) and differ largely in terms of geometry. Some faults are very large (as for example some of the large thrust faults), while some other faults have been modelled as multiple small fault patches. The eastern part of the Swiss molasse basin presents less faults than the western part. This could be due to an interpretation bias, since different groups have been interpreting structures in various sections of the basin. However, the source data being homogeneous (e.g. density of seismic lines) and the fact that much less earthquakes are present in the eastern part of the basin suggest that this lack of fault structures is real (Allenbach et al. 2017). Geological models are not static entities but evolve with new data collection and interpretation. Thus, the assessment of geothermal favorability will also need to be re-assessed when new data becomes available.

Figure 3 : View from GeoMol18 modelled faults (figure produced from viewer.geomol.ch)

2.3 Springs and Thermal Springs

We used existing compilations of thermal and mineralized springs from Sonney and Vuataz (2008) to identify areas where deep-seated fluid flow occurs naturally (Figure 4). We complemented the spring data with information collected from the hydrogeological atlas of Switzerland 1:100000. We identify the presence of major karst springs bordering the swiss plateau, and these springs are typically related with epigenetic karst systems and are not direct indicators of deep-seated fluid flow. However, these karstic systems are often associated with geological structures that favor fluid flow. Typically these structures extend deeper into the sedimentary cover, so we assume that if these structure favor fluid flow near the surface, they may also contribute to deep circulation.

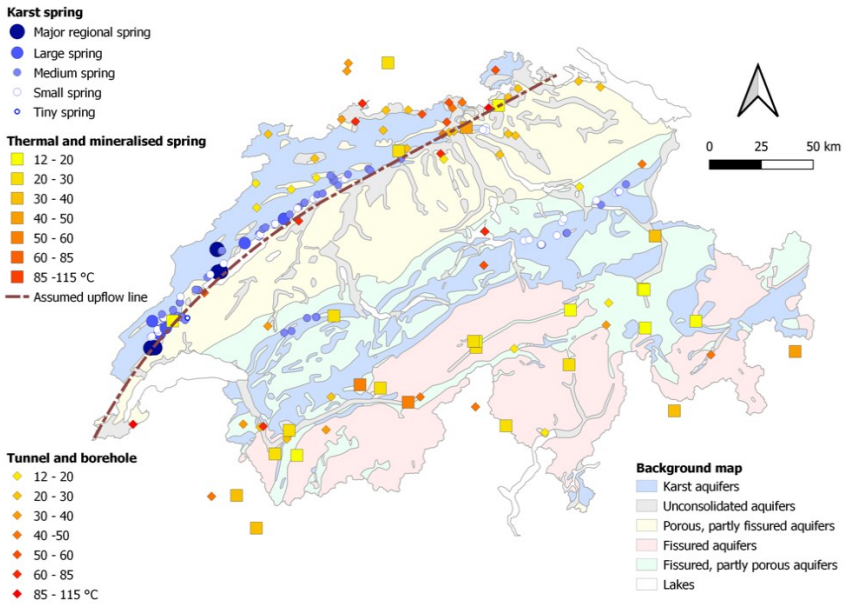

Figure 4 : Hydrogeological data collection including karstic springs and thermal and mineralized springs from Sonney and Vuataz (2008). The map background was downloaded from www.bafu.admin.ch.

2.4 Flow Patterns Beneath the Swiss Plateau

Figure 5 shows a conceptual model of the flow pattern in sedimentary basins (modified after Tóth (1999) and Klimchouk (2011)). Larger recharge occurs over the reliefs and then the flow is gravity-driven towards lower elevations. Depending on the complexity of the topography, flow systems of various scales (local scale, intermediate scale, regional scale) can be nested. In the regions of the Swiss plateau bordered by the Jura mountains to the North and the alps to the South, we can expect that the regional flow systems driven by these topographic highs converge below the Swiss plateau. Flow is predominantly upwards at the convergence point. In an idealized symmetric and homogeneous case, the upwelling area should occur at mid-distance between the two topographic highs. The Swiss plateau differs significantly from this idealized situation because: 1) the topography to the South (Alps) is more pronounced than to the North (Jura) and thus one could expect that the convergence area would be offset to the North; and 2) the hydrogeological structure of the swiss plateau is highly heterogeneous and anisotropic, which influences the flow patterns not only in the sedimentary cover but also in the underlying basement (Kimmeier et al. 1984; Kiraly 1992).

The hydrogeological effects of the fault zones of the Alpine front are not well understood but likely act as hydraulic barriers and isolate flow systems. Assessing these effects requires systematic flow simulations, but this beyond the scope of this paper. For our purposes, we assume that such converging upwelling zones must occur somewhere below the Swiss plateau. This is represented as a line on Figure 4 that runs from SW-NW approximately parallel to the alpine front and the Jura South border. We place this line close to the front of the Jura based on the position of hot and mineralized springs and the overall asymmetric structure of the Molasse basin.

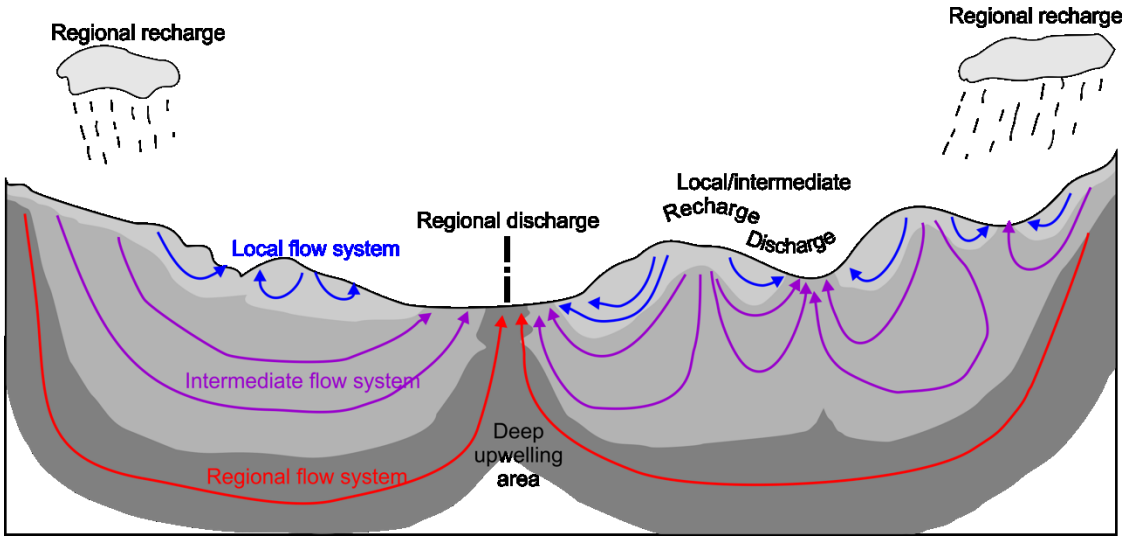

Figure 5 : Conceptual regional, intermediate and local flow field in a basin. Modified after Tóth (1999) and Klimchouk (2011).

2.5 Temperature Field

The GeoMol model includes a 3D temperature field and we use this data in our analyses to identify favorable geothermal targets. Figure 6 shows the depths of 80 °C and 120 °C isotherms, which represents typical minimum target bottom hole temperatures for direct-use heating and electricity productions, respectively. The shallower these isotherms are located, the easier and cheaper it will be to develop a deep geothermal project.

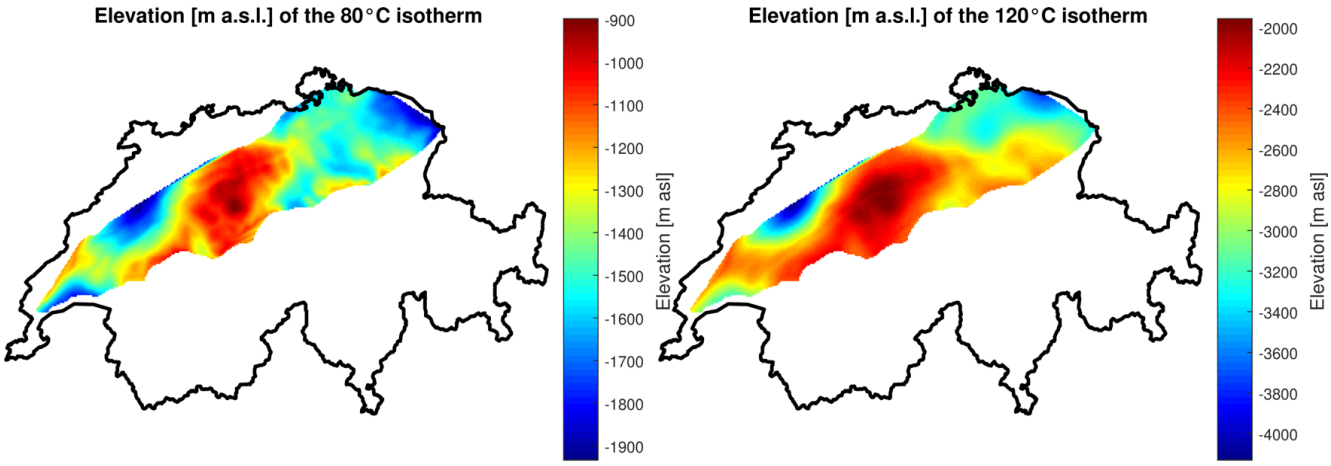

Figure 6 : Elevation (a.s.l.) of the 80 °C and 120 °C isotherm of the GeoMol temperature model.

2.6 Heat Flow Map

Elevated heat flow can be symptomatic of advective heat transport in the upper crust, and Figure 7 shows the Swiss heat flow map compiled by Swisstopo, based on work from Bodmer (1982) and Medici and Rybach (1995).

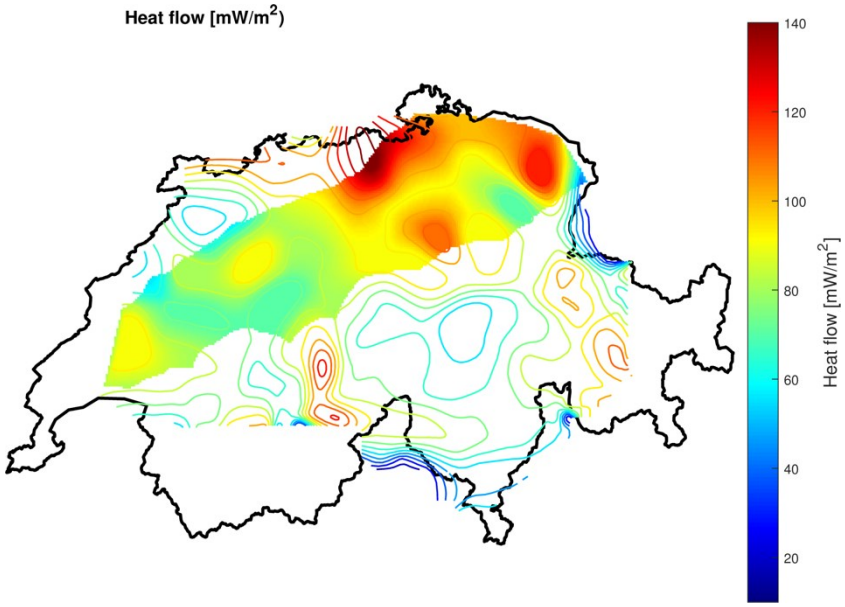

Figure 7 : Heat flow map of Switzerland from swisstopo (geo.admin.ch)

2.7 Stress Field

The stress field in the crust is largely unknown except locally where it can be measured in boreholes (Becker 2000; Heidbach and Reinecker 2003) or estimated from inversion of focal mechanisms (Kastrup et al. 2004). Geostatistical interpolation of sparse stress information is not satisfying. In order to support our geothermal favorability analyses, we perform finite element simulations of the Swiss plateau to develop stress models. Figure 8 shows the model using the geometry from the GeoMol dataset, albeit with some modifications to generate an adequate (computationally feasible) finite element mesh. In particular, layer thickness has a minimum threshold set to 80 m. To avoid boundary effects, we extended the model well beyond the GeoMol area. Outside the domain of interest, the geometry has been modelled as a large-scale monocline that follows the overall trend of the GeoMol model horizon (orientation 150/04). This geometry obviously does not represent reality, but this allows for large buffer zones between the boundaries and the areas of interest.

The stress model measures 320x115 km^2, and extends to 10 km below sea level. The model has an overall trapezoidal shape in order to induce the observed fanning maximum horizontal stress orientation in the Alpine foreland (Becker 2000; Heidbach and Reinecker 2003). In addition, the key feature of the model is an accurate representation of the topography to insure a good estimation of the gravitational stress component. Stiffness contrasts implemented in the model follows the mechanical stratigraphy of Figure 2, and stiff layers attract stress when tectonically loaded. We simulate tectonic loading by imposing displacement boundary conditions. The model is loaded to obtain strike-slip stress regimes in the Molasse Basin, as indicated by focal mechanisms studies (Kastrup et al. 2004) and loaded to critical stress conditions.

We used the RS3 software from Rocscience, and assumed linear elastic rheology for all our layers. The material properties are listed in Table 1. Principal stresses, Von Mises stresses and total stress components were exported and post-processed with MATLAB.

Table 1: Simplified mechanical stratigraphy and properties used for stress modeling

	Molasse	Cretaceous & Malm	Lower jurassic	Upper Dogger	Lower Dogger	Keuper limest.	Gips-keuper	Muschel-kalk	Anhydrite group	Basement
E [GPa]	15	40	15	30	10	20	15	40	5	30
v [-]	0.29	0.25	0.29	0.27	0.29	0.25	0.25	0.25	0.35	0.25

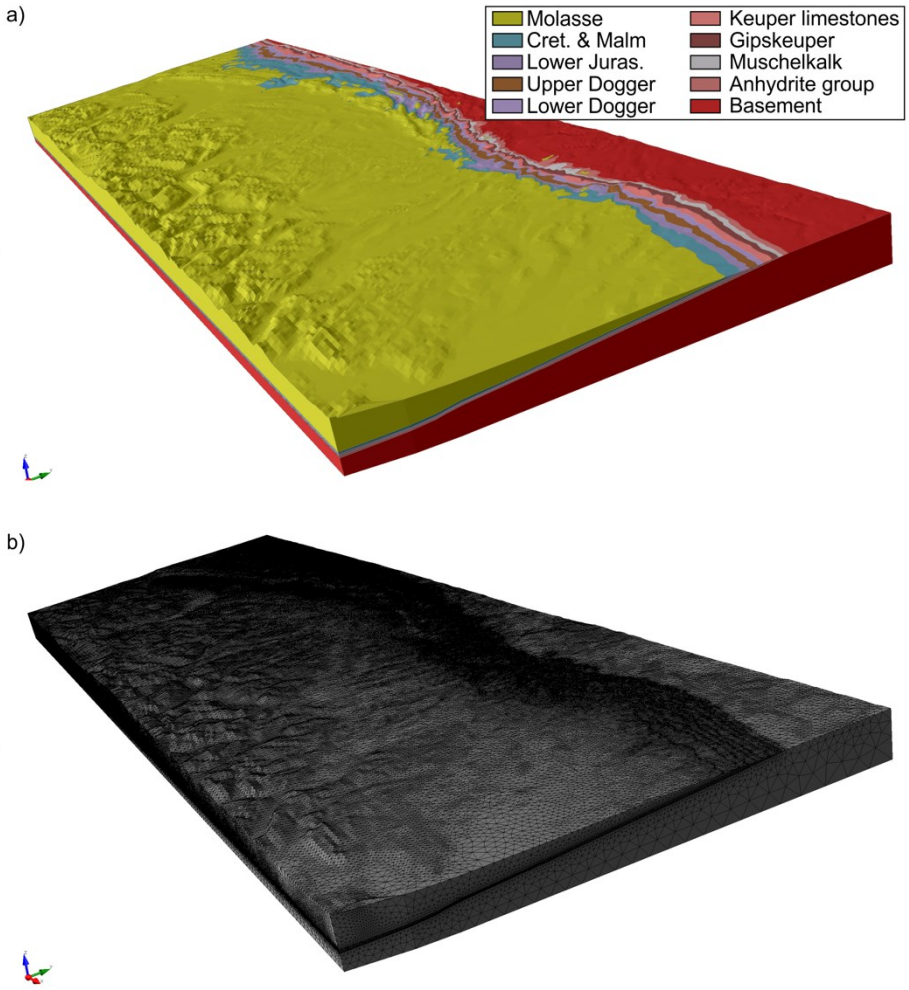

Figure 8 : View of the 3D stress model used in these analyses. a) view of the model with various materials. b) tetrahedral mesh used for the stress analyses.

2.8 Earthquake Catalogue

Earthquake epicenters between 1976-present were downloaded from the Swiss Seismological Survey website, and Figure 9 shows the catalogue for 24603 events. For simplicity, we used the epicenter density as a proxy for deep-seated rock mass damage and associated enhanced permeability.

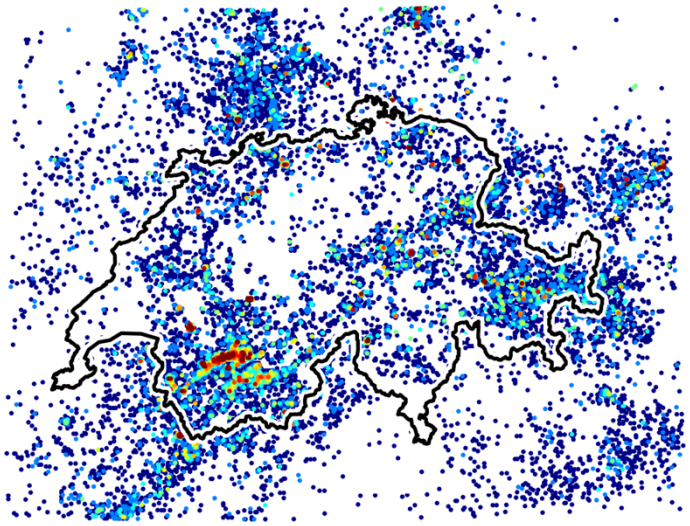

Figure 9 : Epicenters map of the seismic catalog used in this study. Data are colored by point density in order to highlight areas with many overlapping data points.

3 APPROACH

A geothermal 'fairway' is a location favorable for geothermal exploitation. There are two basic requirements to make a geothermal fairway: 1) sufficiently elevated temperature for the targeted use, and 2) sufficient mobility of crustal fluid to be able to extract the heat in an efficient and sustainable manner. The second element requires sufficient rock mass permeability. This can occur either as a primary characteristic (e.g. sufficient connected porosity) or inherited through the rock mass evolution and secondary processes (e.g. fracturing, dissolution). The secondary processes often play the most important role for geothermal fairways in order to generate sufficient connected and permeable rock masses, so brittle structures generating fracturing are often favorable targets. The stress field acting on these structures is also important, as it has been shown that active fluid flow occurs preferentially on critically stressed structures (Barton et al. 1995; Zhang and Sanderson 2001). Following such representation, Siler and Faulds (2013) proposed the following definition for geothermal fairways: "… [a geothermal fairway] occurs where critically stressed fault zones intersect or tip out, are hosted in lithologic units which maximize fracturing and are collocated with elevated heat." Note that in this definition there is no consideration to the surface users, and we agree that with this definition, geothermal fairways should be targeted primarily based on subsurface conditions and not be influenced (at this stage) by surface user considerations. Indeed, previous geothermal development projects driven by user availability and other opportunities at the surface has sometimes led to dry holes.

Following Siler and Faulds (2013) we collected data pertinent to the geothermal fairway definition above. We attributed a score to each component of our dataset, and we call this the *favorability index.* We compute the favorability index with a range between 0 and 1 for each component, with 0 being unfavorable and 1 being favorable for the presence of a geothermal fairway. Finally, we combined all the scores to obtain a consolidated favorability index.

We performed our analyses on a 1km x 1km grid covering the extent of the GeoMol model, focusing on 80 °C and 120 °C because these are the typical minimum temperature levels for direct use and electricity production, respectively. Focusing on these levels allows presenting results in the form of maps. The same approach could have also been applied to any other temperature level or applied directly on a volumetric grid. The list of the criteria used in our favorability analyses and the computation of the favorability index for each grid cell is presented in Table 2.

Table 2: Summary of the criteria used to determine the favorability index.

	Criteria	Unit	Conversion to favorability index [0 unfavorable – 1 favorable]	Weights
1	Depth to target isotherm	m	Linear scale from max(depth)=0 to min(depth)=1	1
2	Surface heat flow	mW/m^2	Linear scale from min(heat flow)=0 to max(heat flow)=1	0.5
3	Seismic event density	$evts/km^2$	Logarithmic scale ceiled a 10 evts per km^2	1
4	Lithology and aquifer thickness	m	=0 if in aquiclude; =normalized aquifer thickness in aquifers	2
5	Distance to faults	m	(dist>1km)=0; (dist<100m)=1; Linearly scaled for (100m<dist<1km)	1
6	Slip tendency on nearest fault	-	Normalized slip tendency for dist. to nearest fault <1km; =0 otherwise	1
7	Dilation tendency on nearest fault	-	Normalized dilation tendency for dist. to nearest fault <1km; =0 otherwise	1
8	Von Mises stress	MPa	Linear scale from min(Von Mises)=0 to max(Von Mises)=1	2
9	Distance to assum. upwelling line	m	Linear scale from (0 km)=1 to (10 km)=0. (>10km)=0	0.5
10	Distance to karst spring	m	Linear scale of distance for dist<2km. (dist>2km)=0	0.5
11	Distance to thermal/mineral. Spring	m	Linear scale of distance for dist<5km. (dist>5km)=0	1

4 RESULTS

Figures 10 to 12 show the complete results for the 80 °C target, while Figure 13 shows only the final combined favorability index for the 120 °C case. For the 80 °C case, the criteria are shown on the left side of the figure, and the derived favorability index for each criterion are presented on the right side of the figure. The combined favorability index is shown on the bottom of Figure 12.

The first criterion that we use is the depth to the target isotherm (Figure 10 top) because drilling costs increase significantly with depth and this is a first-order economic criterion. The depth of the 80 °C isotherm ranges from 1460 m (in the Olten-Araau area) to 3026 m (close to the alpine north front in the eastern part of the country). For simplicity, we linearly rated favorability between these two limits, but more sophisticated rating schemes could be devised and included in future favorability computations.

Elevated heat flow indicates more vigorous heat flow through advective transport, which could indicate deep-seated fluid circulation, so we applied better scores to areas with higher heat flow (Figure 10, second line).

We used the seismic events catalog and computed the number of events per unit area (independent of event depth). This is a difficult rating to give because on the one hand, seismic events identify tectonic deformation and associated rock mass fracturing and associated fluid flow, thus a favorable geothermal target. On the other hand, a more active seismic area might indicated elevated seismic risk and thus a negative geothermal target. We chose to focus on the necessity of rock mass damage and permeability creation for developing deep geothermal resources, and thus gave higher ratings to areas with larger seismic event density. The density in number of events per km^2 spans 3 orders of magnitude, so we use a logarithmic scaling to obtaining sufficient contrast from this criterion (3rd line in Figure 11. This aspect can be expanded in future studies to include depths (if well-constrained) and also magnitude because magnitude identifies the extent of the co-seismic fracturing. In future, we suggest also to include seismic risk evaluation approaches (e.g. Trutnevyte and Wiemer 2017) in the framework of geothermal favorability computations.

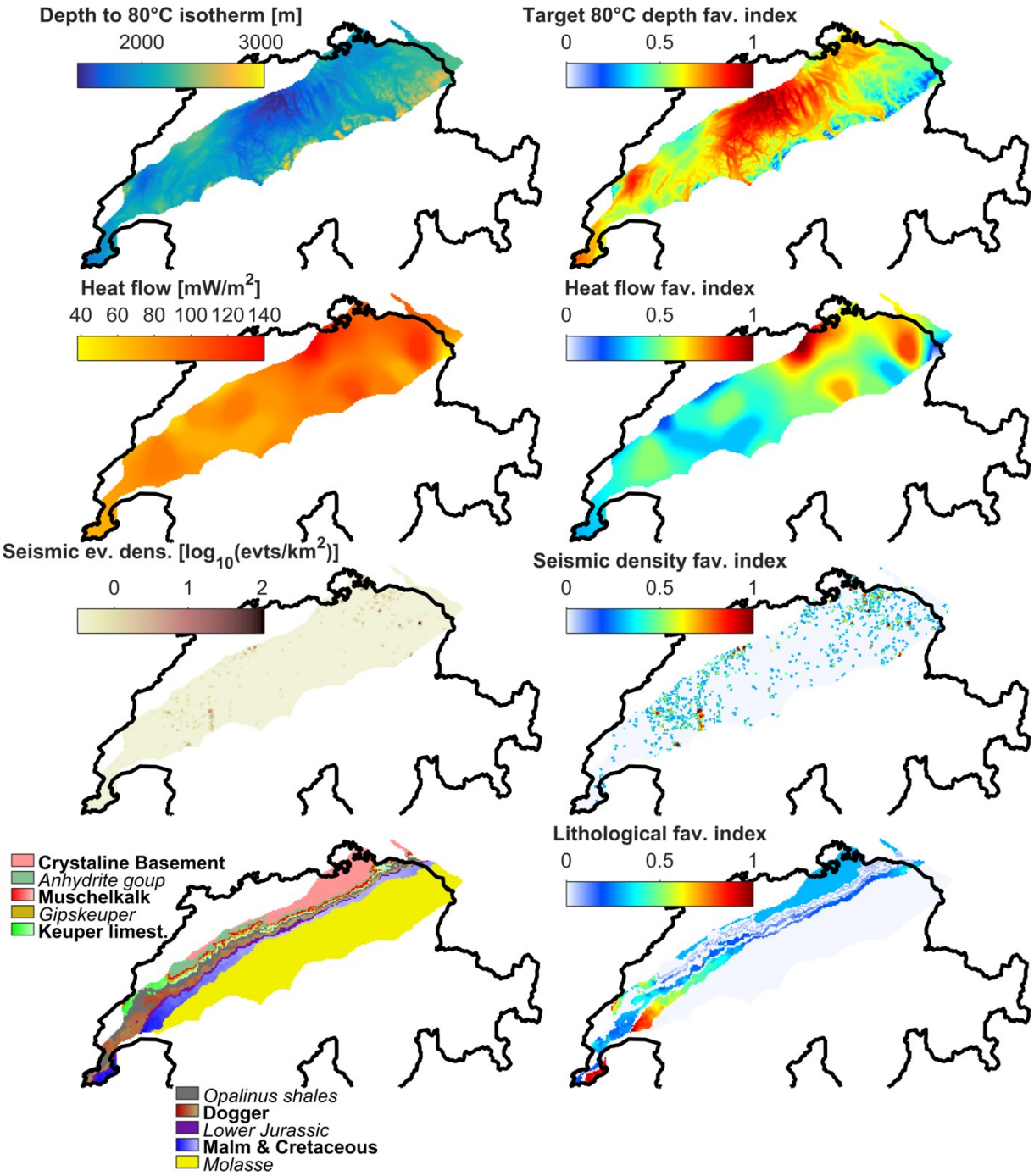

Figure 10 : Details of the first four criteria (left) and their corresponding favorability index (right) for a target at the 80 °C isotherm.

Favorable lithology is a key factor for developing a geothermal project. We intersected the 80°C isotherm with the GeoMol horizons model in order to assess lithology at depth (Figure 10 bottom). We converted this lithological map to favorability index by giving a 0 rating to known aquiclude formations and scaled the favorability index to aquifer thickness for the aquifer formations. We gave a 400 m thickness for basement rock aquifer, representing the fractured, weathered and hydraulically active top-of-basement. Future studies should include lateral facies variability (see for example Adams and Diamond 2019 for the Muschelkalk aquifer) as this can have a large impact on the hydrological and mechanical characteristics of the formations.

The next set of criteria include aspects related to faults and stresses (Figure 11). The presence of faults and high Von Mises stresses indicates rock mass damage favorable for enhanced permeability. Grid cells close to faults or with high Von Mises stresses are thus rated with higher favorability. Stiff formations tend to “attract the stress” which leads to higher differential stress and Von Mises stress, and these are the formations receiving the highest rating. We also computed on all the faults segments the slip and dilation tendency, and gave an elevated favorability index for grid cells located close to faults with high slip or dilation tendency

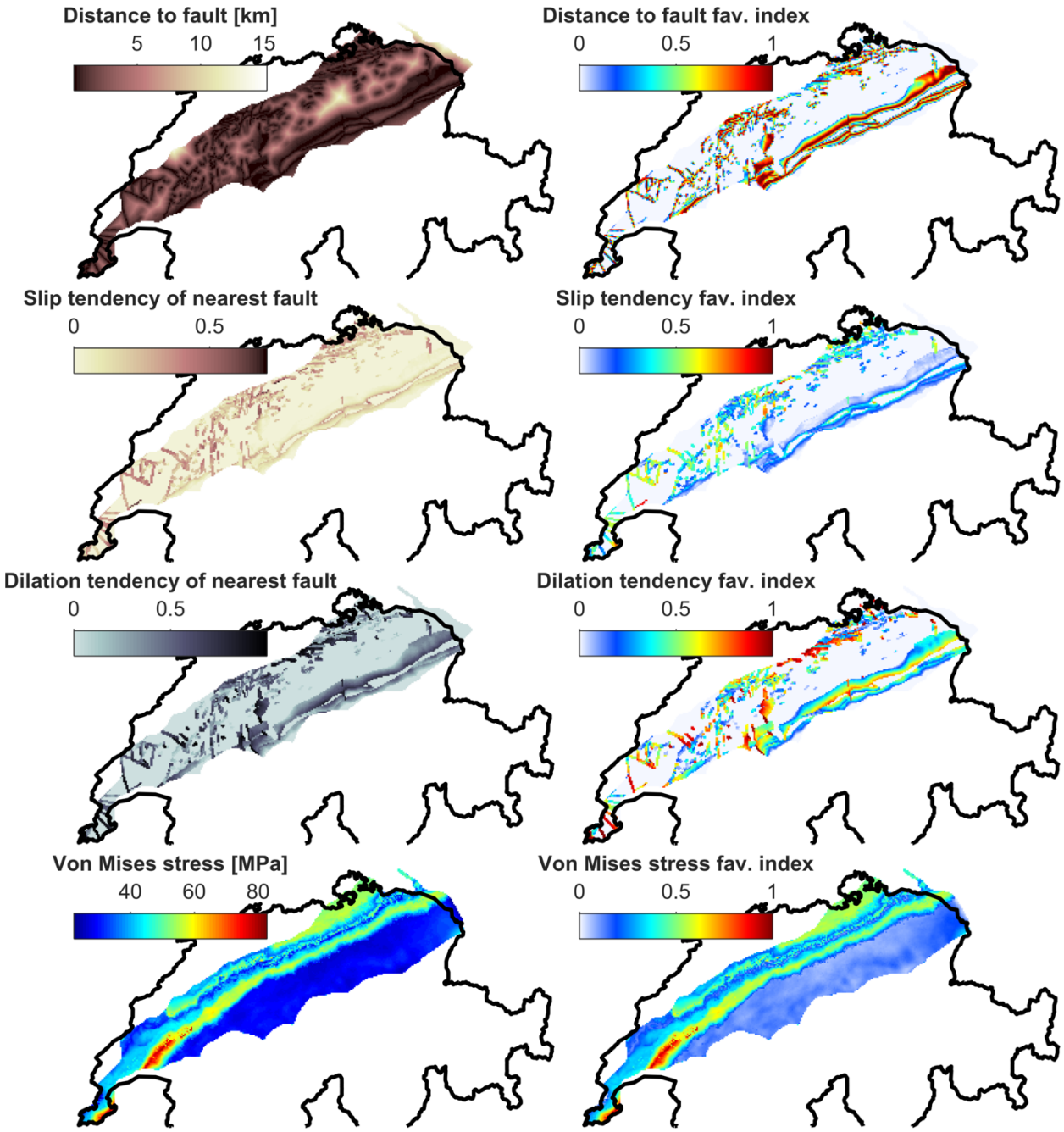

Figure 11 : Details of criteria five to eight (left) and their corresponding favorability index (right) for a target at the 80 °C isotherm.

The last three criteria (Figure 12) concern hydrological indicators, including the distance to karstic springs, to thermal or mineralized spring, and the distance to a basin scale upwelling area. Short distances between these elements are considered favorable for geothermal fairways.

Finally, we combine all these favorability indices, I_i, to generate a combined favorability index I_{comb} (Figure 12, bottom). We used a weighted average scheme to do the combination:

$$I_{comb} = \frac{\sum_{i=1}^{n} I_i w_i}{\sum_{i=1}^{n} w_i} \quad (1)$$

where w_i are the weights attributed to each element. The weights were determined by expert judgement and are listed in Table 2. Ideally, the weight should be defined using a statistical scheme by integrating conditions of actual projects. This can be revised when data from exploration boreholes and projects becomes available.

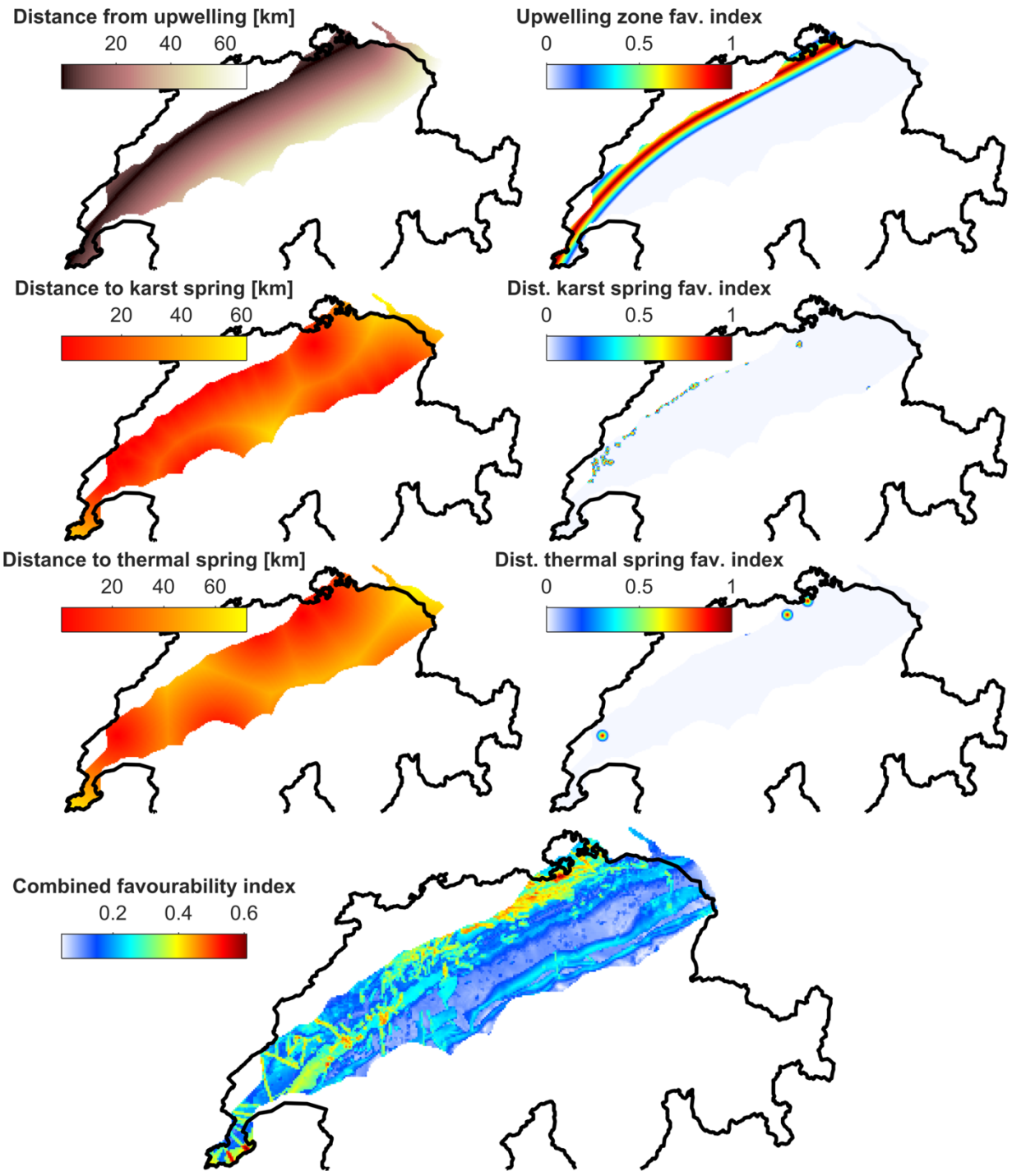

Figure 12 : Details of criteria nine to eleven (left) and their corresponding favorability index (right) for a target at the 80 °C isotherm. Bottom: combined favorability index for the target at 80 °C.

The exact same analyses were performed for the target isotherm 120 °C. The results are presented on Figure 13 in the form of the combined favorability map. Comparing the two maps, there is shift toward the Southeast of the favorable zones due to the influence of aquifer formations within an overall Southeast dipping foreland basin geometry. However, the presence of sub-vertical strike slip faults generate fairways at the same location for both targets.

5 DISCUSSION AND CONCLUSION

The results presented here show that with the available data, sharp contrasts in favorability can be highlighted on the Swiss plateau and these contrasts can guide exploration. However, these results should be considered preliminary because of our simplifying assumptions, the paucity of data, and the scale of Switzerland, which may not be appropriate for local scale exploration planning. Particularly, an attempt should be done to calibrate and validate the approach using appropriate data assimilation techniques. The difficulty is that direct evidence from geothermal projects or deep drilling on the Swiss plateau are sparse. The methodology and approach for generating favorability maps, however, can be applied in future studies with the availability of additional data, more sophisticated modeling and analysis, and findings from future exploration projects.

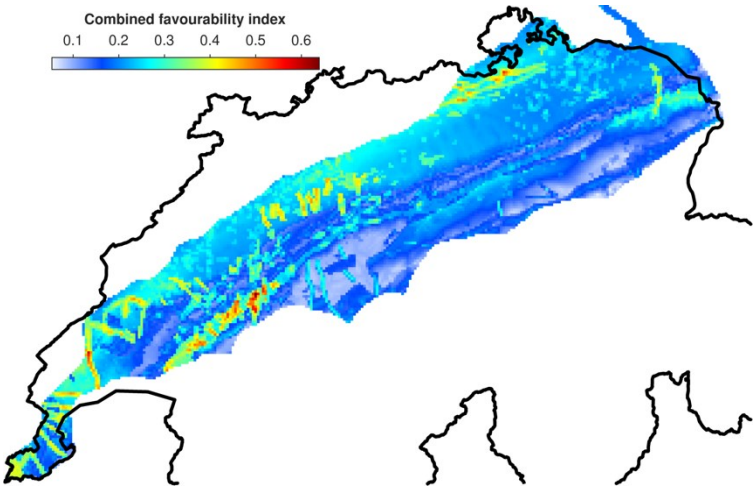

Figure 13 : Combined favorability index for the target at 120 °C

6 ACKNOWLEDGEMENTS

We acknowledge the support from R. Reynolds and R. Allenbach from swisstopo in providing the GeoMol structural and temperature datasets. B. Valley is supported by the Swiss Competence Center for Energy Research SCCER-SoE.

7 REFERENCES

Adams A, Diamond LW (2019) Facies and depositional environments of the Upper Muschelkalk (Schinznach Formation, Middle Triassic) in northern Switzerland. Swiss J Geosci. https://doi.org/10.1007/s00015-019-00340-7

Allenbach R, Baumberger R, Kurmann E, et al (2017) GeoMol: Modèle géologique 3D du bassin molassique suisse – rapport final. Rapp. Serv. géol. natl. 10 FR

Barton C, Zoback M, Moos D (1995) Fluid flow along potentially active faults in crystalline rock. Geology 23:683–686

Becker A (2000) The Jura Mountains — an active foreland fold-and-thrust belt? Tectonophysics 321:381–406. https://doi.org/10.1016/S0040-1951(00)00089-5

Bodmer P (1982) Geothermische Karte der Schweiz / Carte géothermique de la Suisse. Schweizerischen Geophysikalischen Kommission

Burkhard M, Sommaruga A (1998) Evolution of the western Swiss Molasse basin: structural relations with the Alps and the Jura belt. Geol Soc Lond Spec Publ 134:279–298. https://doi.org/10.1144/GSL.SP.1998.134.01.13

Chevalier G, Diamond LW, Leu W (2010) Potential for deep geological sequestration of CO2 in Switzerland: a first appraisal. Swiss J Geosci 103:427–455. https://doi.org/10.1007/s00015-010-0030-4

Heidbach O, Reinecker J (2003) Analyse des rezenten Spannungsfelds der Nordschweiz. Nagra

Hergert T, Heidbach O, Reiter K, et al (2015) Stress field sensitivity analysis in a sedimentary sequence of the Alpine foreland, northern Switzerland. Solid Earth 6:533–552. https://doi.org/10.5194/se-6-533-2015

Kastrup U, Zoback ML, Deichmann N, et al (2004) Stress field variations in the Swiss Alps and the northern Alpine foreland derived from inversion of fault plane solutions. J Geophys Res 109:

Kimmeier F, Perrochet P, Andrews R, Kiraly L (1984) Simulation par Modèle Mathématique des Ecoulements Souterrains entre les Alpes et la Forêt Noire. Nagra

Kiraly L (1992) Hydrodynamics of the Swiss Molasse basin. In: Symposium on Swiss Molasse Basin

Klimchouk A (2011) Hypogene Speleogenesis: hydrogeological and morphogenetic perspective. National Cave and Karst Research Institute

Medici F, Rybach L (1995) Geothermal map of Switzerland 1995 (heat flow density). Schweizerischen Geophysikalischen Kommission. Publication Nr 30.

Siler DL, Faulds JE (2013) Three-Dimensional Geothermal Fairway Mapping: Examples From the Western Great Basin, USA. GRC Trans 37:327–332

Sonney R, Vuataz F-D (2008) Properties of geothermal fluids in Switzerland: a new interactive database. Geothermics 37:496–509

Tóth J (1999) Groundwater as a geologic agent: An overview of the causes, processes, and manifestations. Hydrogeol J 7:1–14. https://doi.org/10.1007/s100400050176

Trutnevyte E, Wiemer S (2017) Tailor-made risk governance for induced seismicity of geothermal energy projects: An application to Switzerland. Geothermics 65:295–312. https://doi.org/10.1016/j.geothermics.2016.10.006

Zhang X, Sanderson DJ (2001) Evaluation of instability in fractured rock masses using numerical analysis methods: Effects of fracture geometry and loading direction. J Geophys Res Solid Earth 106:26671–26687. https://doi.org/10.1029/2001JB000311